Material parameters and thermal stability of synthetic ferrimagnet free layers in magnetic tunnel junction nanopillars

D. Markó,[1,2,a)] T. Devolder,[1,2] K. Miura,[3,4] K. Ito,[3,4] Joo-Von Kim,[1,2] C. Chappert,[1,2] S. Ikeda,[4,5] and H. Ohno[4,5]
[1]*Institut d'Electronique Fondamentale, Université Paris-Sud 11, 91405 Orsay, France*
[2]*UMR 8622, CNRS, 91405 Orsay, France*
[3]*Hitachi, Ltd., Advanced Research Laboratory, 1-280 Higashi-koigakubo, Kokubunji-shi, Tokyo 185-8601, Japan*
[4]*Laboratory for Nanoelectronics and Spintronics, Research Institute of Electrical Communication, Tohoku University, 2-1-1 Katahira, Aoba-ku, Sendai 980-8577, Japan*
[5]*Center for Spintronics Integrated Systems, Tohoku University, 2-1-1 Katahira, Aoba-ku, Sendai 980-8577, Japan*

(Received 26 June 2012; accepted 9 August 2012; published online 13 September 2012)

We have determined the material parameters of optimized synthetic ferrimagnet (SyF) free layers in magnetic tunnel junctions by means of magneto-resistance loops as well as microwave noise spectroscopy under constant voltage, and the field dependence thereof. By comparing the experimental data with calculated loops and spin wave modes from a 2-macrospin model, we have deduced the saturation magnetization, anisotropy, damping, and interlayer exchange coupling. From waiting time experiments of field-induced switching, the energy barrier relevant for the thermally activated switching of the free SyF has been experimentally evaluated and compared to an existing model in order to assess its consistency. © *2012 American Institute of Physics*. [http://dx.doi.org/10.1063/1.4751025]

I. INTRODUCTION

Synthetic antiferromagnets (SAFs) and synthetic ferrimagnets (SyFs)[1,2] are trilayers consisting of two thin ferromagnetic layers with equal, respectively, different magnetic moments that are antiferromagnetically coupled via RKKY interaction by an ultrathin, nonmagnetic metallic spacer. These kinds of structures have unique properties making them interesting for applications in magnetic data storage or sensor technology. For instance, the weak net moment and small stray field of SyFs minimize magnetostatic interactions between adjacent magnetic elements such as magnetic tunnel junctions (MTJs) or spin-valves. Moreover, compared to isolated ferromagnetic layers, SyFs have a higher coercivity and a lower ratio of switching current density to thermal stability factor.[3] In order to optimize SyFs for a given application, the exact knowledge of their materials parameters and the corresponding influence on the critical fields (spin-flop field, direct-write field, and saturation field) are indispensable. Here, we present combined experimental and theoretical studies of in-plane magnetized SyFs, which are used as free and reference layers in MgO-based MTJs. Combining *R–H* loops measurements as well as microwave noise spectroscopy, and using a 2-macrospin model, we will extract the magnetic parameters of the free SyF. Moreover, from waiting time experiments of field-induced switching, the energy barrier relevant for the thermally activated switching will be experimentally evaluated and compared to an existing model.

a)Electronic mail: daniel.marko@ief.u-psud.fr.

II. SAMPLE COMPOSITION

Fig. 1(a) shows a sketch of the investigated MTJ nanopillars, where the thickness of the individual layers in nm is given by the numbers in parenthesis. The trilayer above (below) the 0.85 nm thick MgO tunnel barrier represents the free (reference) SyF. The purpose of the small MgO layer on top of the free SyF is to provide a surface anisotropy contribution that lowers its effective magnetization. The thickness x of the Ru spacer varies between 0 and 1.5 nm, leading to a different type (ferromagnetic or antiferromagnetic) and strength of interlayer exchange coupling. For the samples investigated in this study, the value was approximately 0.9 nm, which leads to weak antiferromagnetic coupling. The stacks have been patterned into rectangles having a lateral size $L_x \times L_y$ of 200×100 nm^2, with the exchange bias direction of the IrMn antiferromagnet being parallel to the long side, which represents the easy axis of magnetization as well. In the parallel (P) and antiparallel (AP) states, the MTJs typically have resistances in the range of 2 kΩ, corresponding to a resistance–area product of 40 $\Omega\,\mu$m^2.

III. RESULTS AND DISCUSSION

A. Material parameters

The normalized resistance R of a typical MTJ as a function of an applied magnetic field H along both easy and hard axis is depicted in Figs. 1(c) and 1(e), respectively. The easy axis curve shows that the MTJ possesses both low and high resistance P and AP states and three critical fields. These are the direct-write field $\mu_0 H_{dw}$ at a value of ±21 mT, the spin-flop field $\mu_0 H_{sf}$ at ±27 mT, and the saturation field $\mu_0 H_{x,sat}$

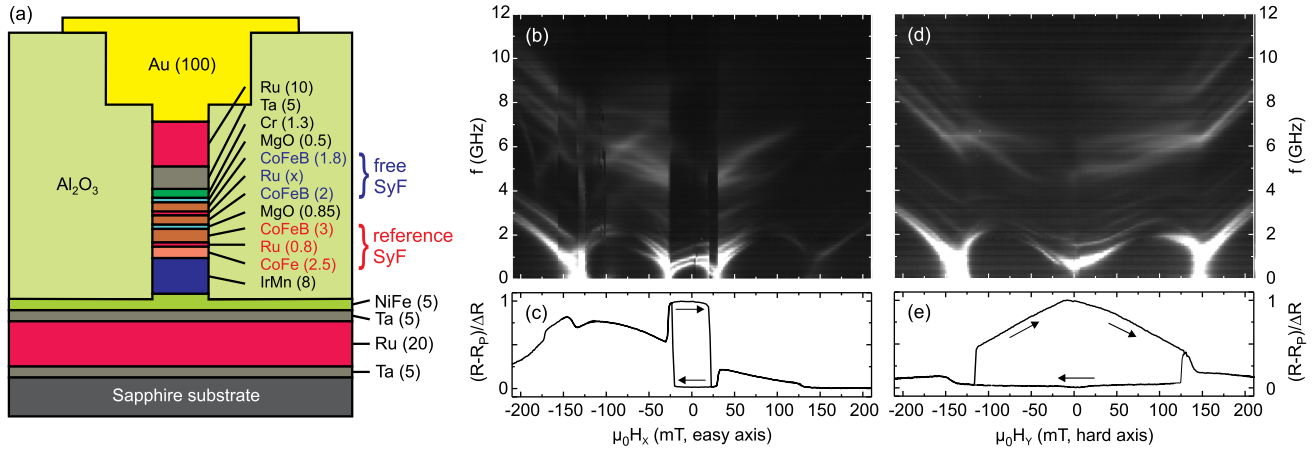

FIG. 1. Composition of the MTJ nanopillars (a) as well as typical power spectrum densities (for decreasing field, log scale) and *R–H* loops of MTJ nanopillars with SyF reference and SyF free layers for a magnetic field applied along easy (panels (b) and (c)) and hard (panels (d) and (e)) axis, respectively.

at a value of ± 143 mT. The asymmetry of the loop and the decrease of the resistance in the negative field range for values smaller than $\mu_0 H_x = -143$ mT arise from the influence of the exchange-biased reference SyF. From the hard axis loop, one can see that there are also two AP states at zero field, but only one low resistance P state at high fields. With ± 145 mT, the hard axis saturation field $\mu_0 H_{y,sat}$ is slightly larger than $\mu_0 H_{x,sat}$. From both saturation fields, which in the case of a SAF are given by[4]

$$\mu_0 H_{x,sat} = \mu_0 H_J - \mu_0 H_k, \tag{1}$$

$$\mu_0 H_{y,sat} = \mu_0 H_J + \mu_0 H_k, \tag{2}$$

one can give a first estimate of the interlayer exchange coupling field $\mu_0 H_J$ and uniaxial anisotropy field $\mu_0 H_k$, whose values are 145 mT and 1 mT, respectively.

To record spin-wave eigenspectra of the MTJs, we have performed microwave noise spectroscopy,[5,6] where the current-noise power spectrum density (PSD) as a function of the applied magnetic field was measured for small bias voltages. In the noise spectra (Figs. 1(b) and 1(d)), white regions correspond to maxima in the PSDs and thus to eigenexcitations of the SyFs. Upon choosing a suitable value for the bias voltage, one has to find a trade-off between a value high enough to provide a decent signal-to-noise ratio and a value low enough not to affect the eigenmode frequencies by spin transfer torque, Oersted field, or Joule heating. All MTJs have been measured at $V_{bias} = \pm 250$ mV, a value for which differences in the eigenmode frequencies for opposite voltage polarity amount to less than a few tens of MHz, and differences in the amplitude of the PSD are hardly visible.

The eigenspectra show several modes with significantly different intensities from both the reference SyF and the free SyF. However, we only need to identify the quasi-uniform acoustic and optic modes of the free SyF, for instance, by using their opposite curvatures with respect to the applied field. The low-frequency uniform acoustic mode can be assigned unambiguously, as it is the mode with the lowest frequency and the highest intensity having minima at the critical fields. In the case of the high-frequency uniform optic mode of the free SyF, the situation is less clear. This is due to similar intensities of the modes for frequencies above 4 GHz as well as a possible hybridization of optic and acoustic modes near their crossing, as observed in Ref. 7. Since even subsequently analyzing and processing the eigenspectra in order to extract the different eigenmodes (see Fig. 2(c)) does not allow for a correct assignment, we mainly focus on the acoustic mode. To extract the material parameters of the free SyF, a 2-macrospin model was used to fit the experimental data. The model includes Zeeman, interlayer exchange coupling, dipolar coupling, demagnetizing as well

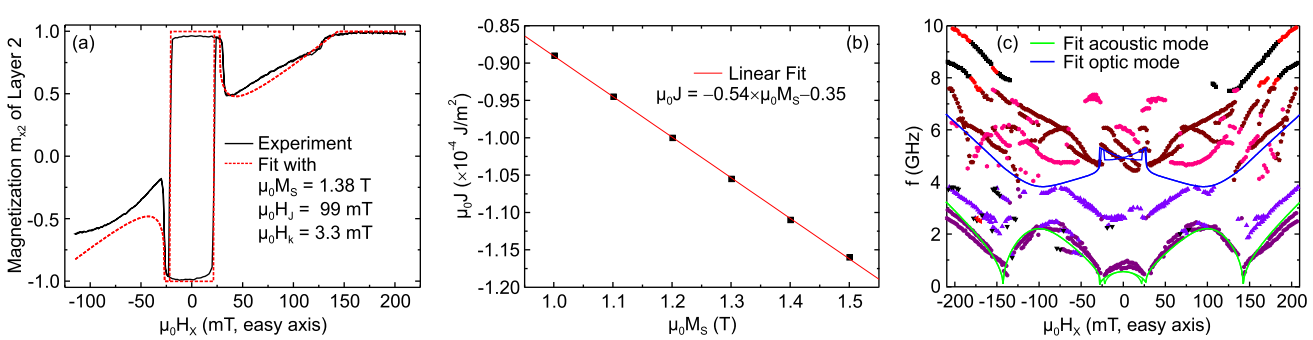

FIG. 2. (a) Experimentally measured $\sigma - H$ loop (solid line) and calculated hysteresis loop (dashed line) of m_{x2} using a 2-macrospin model. (b) Correlation between $\mu_0 J$ and $\mu_0 M_S$ in order to obtain identical fits of the $\sigma - H$ loop. (c) Extracted eigenmode frequencies (symbols) from the easy axis PSD shown in Fig. 1(b) as well as the calculated uniform acoustic and optic mode (lines) of the free SyF.

as in- and out-of-plane anisotropy terms, but disregards damping and spin torque. The free SyF is described by two magnets of thickness $t_1 = 1.8$ nm and $t_2 = 2.0$ nm (the index 1 or 2 refers to the top or bottom layer, respectively) with the magnetization M_S and the uniaxial in-plane anisotropy field H_k. We assume these quantities to be the same for both CoFeB layers, as they differ only slightly in thickness. The antiferromagnetic coupling of both layers is described by the interlayer exchange coupling constant $J < 0$. The corresponding interlayer exchange field is defined as

$$H_J = -\frac{2J}{M_S t_2}, \tag{3}$$

where the choice of normalization with respect to t_2 is arbitrary. The interface anisotropy constant K_s is set to 1.3 $\mathrm{mJ/m^2}$,[8] leading to an effective magnetization

$$M_{\mathrm{eff}} = M_S - \frac{2K_s}{\mu_0 M_S t_1}. \tag{4}$$

The demagnetizing factors N_1^x, N_1^y, N_1^z, N_2^x, N_2^y, and N_2^z of the two ferromagnetic layers have been exactly calculated from Ref. 9, whereas for the mutual dipolar coupling factors N_{12}^x, N_{12}^y, and N_{12}^z, an approximation[10] was used. With exactly calculated mutual dipolar coupling factors from Ref. 11, which are smaller by a factor of 1.5, it is not possible to fit the experimental data, as the values of both the spin-flop and direct-write field are to large and cannot be sufficiently reduced by any combination of the fit parameters. In the following, we describe the fitting procedure in order to extract M_S, J, and H_k from the experimental data. First, we convert the measured resistance R as a function of the applied magnetic field into conductance $\sigma = 1/R$, as only the latter is proportional to the magnetization component m_{x2} of layer 2. Second, we disregard the part of the hysteresis containing the influence of the exchange-biased reference SyF, i.e., all data points for negative fields exceeding $\mu_0 H_x = -115$ mT. This step is necessary since we use the quadratic difference between experimental data and calculated magnetization component m_{x2} at each field step as the quantity to be minimized in order to obtain the best fit. As depicted in Fig. 2(a), there is a very good agreement between experiment and theory, as not only the shape of the $\sigma - H$ loop but also the values of the critical fields can be accurately reproduced. However, there is in principle an unlimited number of pairs of J and M_S giving rise to the same fit loop, as the interlayer exchange field H_J depends on the ratio of J/M_S (see Eq. (3)). Possible combinations of J and M_S as well as the equation relating both quantities are shown in Fig. 2(b). The corresponding values of $\mu_0 H_J$ are not constant, but vary in the range of 97 to 112 mT due to the offset of the fit equation, which is caused by the dipolar coupling. The fact, that the loop shape and the critical fields are not affected by this, can be understood in such a way that the influence of the (antiferromagnetic) dipolar coupling can compensate for the change of H_J. In order to determine the correct pair of J and M_S, the eigenmode spectra have to be fitted as well, since at zero magnetic field the difference between the frequency-squared of the uniform optic and the uniform acoustic mode of the free SyF linearly depends on M_{eff}:[4]

TABLE I. Material and geometry parameters of the free SyF used to fit the $\sigma - H$ loop and the uniform acoustic mode of the eigenmode spectrum shown in Figs. 2(a) and 1(b), respectively. Extracted parameters are shown in bold font.

Parameters		Values
Saturation magnetization	$\mu_0 M_S$	(1.38 ± 0.05) T
Effective magnetization	$\mu_0 M_{\mathrm{eff}}$	(0.2 ± 0.1) T
Interlayer exchange coupling constant	$\mu_0 J$	$(-1.09 \pm 0.04) \times 10^{-4}$ J/m^2
Uniaxial in-plane anisotropy field	$\mu_0 H_k$	(3.3 ± 0.3) mT
Effective damping parameter	α_{eff}	0.009 ± 0.001
Perpendicular anisotropy constant	K_s	1.3 mJ/m^2
Lateral pillar dimensions	L_x, L_y	200 nm, 100 nm
CoFeB layer thicknesses	t_1, t_2	1.8 nm, 2.0 nm
Demagnetizing factors	(N_1^x, N_1^y, N_1^z)	(0.0142, 0.0291, 0.9566)
	(N_2^x, N_2^y, N_2^z)	(0.0155, 0.0317, 0.9528)
Mutual dipolar coupling constants	$(N_{12}^x, N_{12}^y, N_{12}^z)$	(0.0149, 0.0304, −0.0453)
Gyromagnetic ratio	$\gamma_0 = \mu_0 \gamma$	221300 m/As

$$\omega_{opt}^2 - \omega_{ac}^2 = \gamma_0^2 H_J M_{\mathrm{eff}}. \tag{5}$$

In Fig. 2(c), all modes extracted from the easy axis noise spectrum and the calculated uniform modes of the free SyF are depicted. Its low-frequency uniform acoustic mode can be modeled very well, except for fields exceeding $\pm H_{x,\mathrm{sat}}$, where the frequency of the calculated mode is a slightly too high. A summary of the extracted material parameters including their errors is given in Table I.

In addition to M_S, J, and H_k, we have also determined the effective damping parameter α_{eff} of the CoFeB layers constituting the free SyF. For this purpose, we measured the frequency linewidth of the uniform acoustic mode at zero magnetic field, which is given by[4]

$$\Delta\omega_{ac} = \Delta\omega_{opt} = \alpha_{\mathrm{eff}} \gamma_0 (2H_k + H_J + M_{\mathrm{eff}}). \tag{6}$$

The full width at half maximum linewidth is $\Delta\omega_{ac,opt} = 484 \pm 69$ MHz, which gives an effective damping parameter $\alpha_{\mathrm{eff}} = 0.009 \pm 0.001$, that is slightly higher than the bulk value of CoFeB reported in Ref. 12.

B. Thermal stability

The thermal stability of the MTJs has been investigated by means of waiting time experiments conducted in the following way. First, the samples were saturated along their easy axis with a negative field, which was subsequently reduced to zero in a single step in order to prepare a well defined magnetic state. In a second step, the magnetic field was set to various positive values close to, but always below the direct-write field of the free SyF. Finally, the time elapsed till the MTJ switches is then recorded. In Figs. 3(a) and 3(b), the measured waiting times for two different values of the applied field $\mu_0 H_x$ are shown. They follow an exponential distribution, with a mean switching time that exponentially decreases when approaching the direct-write field. The relation between the

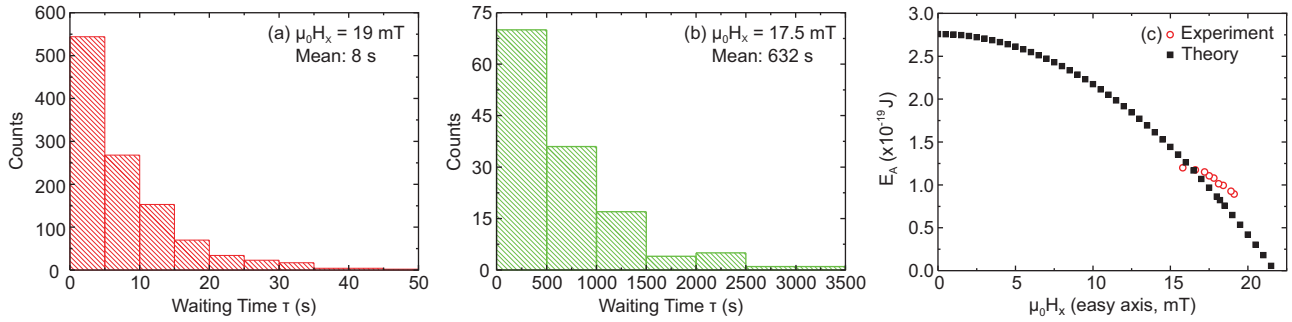

FIG. 3. Panels (a) and (b): Distribution of the waiting times for different values of the applied magnetic field. Panel (c): Energy barrier of the free SyF vs. applied magnetic field as calculated from the waiting times (○) and from its experimentally determined material parameters (■).

waiting time τ and the activation energy E_A of the free SyF is given by the Néel-Arrhenius equation[13]

$$\tau = \tau_0 \ e^{E_A/k_BT}, \tag{7}$$

where $\tau_0 = 10^{-9}$ s is the attempt time. Alternatively, E_A can also be determined from the material parameters and the effective magnetic volume of the free SyF using a model developed by Worledge:[14]

$$\frac{E_A}{\mu_0 M_S L_x L_y (t_1 + t_2)} = \mu_0 \left(H_k - \frac{H_x^2}{H_{x,sat}} \right). \tag{8}$$

In Fig. 3(c), the activation energy as a function of the applied magnetic field, calculated in these two different ways, is shown. The values of E_A calculated from the waiting times are in most cases a bit larger than the ones derived using the material parameters, but they are well within the same range. We attribute this difference to the fact, that the waiting time experiments have been conducted on a sample different from the one, which was used for the determination of the material parameters. However, from a comparison of the corresponding *R–H* loops, both samples are very similar in terms of their material parameters. The zero-field activation energy of the free SyF amounts to 2.8×10^{-19} J, which is equivalent to 67 k_BT at room temperature. This value is identical to the one determined by Hayakawa *et al.*[3] on very similar samples, but using a different experimental technique.

IV. CONCLUSION

In summary, we have extracted the material parameters of SyF free layers in MgO-based MTJ nanopillars. First, we modeled the *R–H* loops, which gives H_k as well as numerous pairs of J and M_S, out of which the correct one can be found by subsequently fitting spinwave spectra. For further improving the model, possible nonuniform magnetization configurations in the free SyF, the influence of the reference SyF as well as damping and spin torque contributions will have to be taken into account. In addition, we have investigated the thermal stability of the free SyF by means of waiting time experiments of field-induced switching. Comparing their results with a model developed by Worledge, which uses the material parameters of the free SyF, we get a good agreement between experiment and theory, which allows to extract the zero-field energy barrier of the free SyF.

This work was supported by the Marie Curie Initial Training Network "SemiSpinNet," financed by the FP7 of the European Commission (Contract-No. MCITN-215368-2), and by the FIRST program from JSPS.

[1]D. Heim and S. S. P. Parkin, "Magnetoresistive spin valve sensor with improved pinned ferromagnetic layer and magnetic recording system using the sensor," U.S. patent 5,465,185 (1995).
[2]H. Van den Berg, "Magnetoresistive sensor having at least a layer system and a plurality of measuring contacts disposed thereon, and a method of producing the sensor," U.S. patent 5,686,838 (1997).
[3]J. Hayakawa, S. Ikeda, Y. M. Lee, R. Sasaki, T. Meguro, F. Matsukura, H. Takahashi, and H. Ohno, Jpn. J. Appl. Phys. Part 2 **45**, L1057 (2006).
[4]T. Devolder and K. Ito, J. Appl. Phys. **111**, 123914 (2012).
[5]T. Devolder, P. Crozat, C. Chappert, J. Miltat, A. Tulapurkar, Y. Suzuki, and K. Yagami, Phys. Rev. B **71**, 184401 (2005).
[6]A. Helmer, S. Cornelissen, T. Devolder, J.-V. Kim, W. van Roy, L. Lagae, and C. Chappert, Phys. Rev. B **81**, 094416 (2010).
[7]M. Belmeguenai, T. Martin, G. Woltersdorf, G. Bayreuther, V. Baltz, A. K. Suszka, and B. J. Hickey, J. Phys.: Condens. Matter **20**, 345206 (2008).
[8]S. Ikeda, K. Miura, H. Yamamoto, K. Mizunuma, H. D. Gan, M. Endo, S. Kanai, J. Hayakawa, F. Matsukura, and H. Ohno, Nature Mater. **9**, 721 (2010).
[9]A. Aharoni, J. Appl. Phys. **83**, 3432 (1998).
[10]A. J. Newell, W. Williams, and D. J. Dunlop, J. Geophys. Res. **98**, 9551, (1993).
[11]O. Fruchart and B. Dieny, J. Magn. Magn. Mater. **324**, 365–368 (2012).
[12]C. Bilzer, T. Devolder, J.-V. Kim, G. Counil, C. Chappert, S. Cardoso, and P. P. Freitas, J. Appl. Phys. **100**, 053903 (2006).
[13]L. Néel, C. R. Acad. Sci. **228**, 664 (1949).
[14]D. C. Worledge, Appl. Phys. Lett. **84**, 4559 (2004).